# Double three-phase PMSM structures for fail operational control

**M. Kozovsky** * **P. Blaha** **

Brno University of Technology CEITEC
Purkynova 123
Brno 612 00, CZECH REPUBLIC

* *Phone: +420 54114 9845*
*(e-mail:matus.kozovsky@ceitec.vutbr.cz)*
** *Phone: +420 54114 6427*
*(e-mail:petr.blaha@ceitec.vutbr.cz)*

**Abstract:** This paper deals with permanent magnet synchronous motors (PMSM) structures. Especially their double three-phase arrangements are analysed in detail. Comparison of three different structures is treated. Non-overlapping concentrated winding is the first analysed structure. Distributed winding arrangement with interlaced sub-systems and also distributed winding arrangement with segregated sub-systems follows.
The behaviour of all motor structures during normal operation is the same but the properties during faults are different. The motor behaviour during active short circuit (ASC) is discussed. ASC of whole motor and also partial ASC tests were performed. Current waveforms in different operating points are compared. Results show differences of individual structures with respect to operation during fault.

*Keywords:* Double three-phase motor, Multi-phase motor, PMSM, Motor structure.

## 1. INTRODUCTION

The motor behaviour depends especially on motor parameters. Mutual inductances and motor symmetry is defined by stator construction. Stator can be constructed using several different methods. Stator arrangements analysis is important for controller design. Some motor arrangements can be fail safe in some cases, however faults can significantly affect the whole system. The example is the motor which is not able to generate sufficient power anymore.

### *1.1 Non-overlapping concentrated winding*

Non-overlapping concentrated winding is one possible stator arrangement. Each coil is rotated around one tooth. Coils are connected in series or in parallel to create individual phase windings A,B and C of three-phase motors. Back-EMF waveforms are displaced by 120 degrees electrical Dhulipati et al. (2017). Double or triple three-phase motor can be also created easily using this method. Coils are evenly distributed into individual sub-systems to form multiple three-phase systems Giangrande et al. (2019). Back-EMF waveforms are shifted by 120 degrees electrical within individual sub-systems. However back-EMF phase shift between sub-systems can exist.

The advantage of this arrangement comes from low mutual inductances between sub-systems. Mutual inductances between sub-systems can help to improve motor behaviour during some faults. But on the other side, mutual inductance can cause problems during different faults. From the symmetry point of view, individual sub-systems are typically symmetrical using non-overlapping concentrated winding arrangement. Control algorithms used for three-phase motors can be used also for individual three-phase subsystems of multiple three phase motor. However asymmetric structure can be also created Yepes et al. (2017)

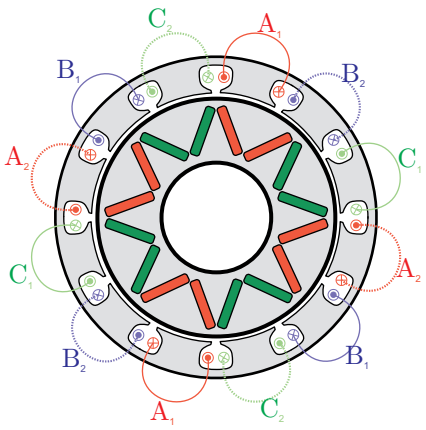


Fig. 1. Double three-phase motor with non-overlapping concentrated winding and interlaced sub-systems.

Winding factor when using non-overlapping concentrated winding is typically lower comparing with distributed winding arrangement Chong et al. (2010). This disadvantage can be partially compensated using proper pole-pairs number and stator slots combination. Figure 1 shows motors with non-overlapping concentrated winding. This arrangement is also defined as motor with interlaced sub-systems, because each coil of first sub-system is located next to the coil of another one.

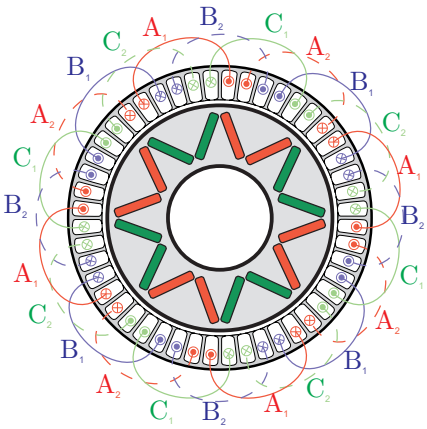


Fig. 2. Double three-phase motor with distributed winding and interlaced sub-systems.

Field weakening index (FWI) is another important parameter of the motor. This parameter is defined as the ratio of the characteristic current $I_{ch}$ over the maximal allowed motor current $I_s$ defined by (1). The $I_s$ is also defined as rated current EL-Refaie (2010).

$$FWI = \frac{I_{ch}}{I_s} \tag{1}$$

The characteristic current $I_{ch}$ is defined as the ratio of magnet flux linkage, $\lambda_m$, to $d$-axis inductance, $L_d$ according to (2). $I_{ch}$ is also the center of voltage-limit ellipse in the rotor referred $dq$ current plane. Rated current is defined as maximum allowed stator current $I_s$, see Pouramin et al. (2017).

$$I_{ch} = \frac{\lambda_m}{L_d} \tag{2}$$

The field weakening index defines machine performance in the field weakening area. For instance, when $I_{ch}$ is equal to the rated current of a PMS machine (FWI = 1), the constant power region can be extended theoretically to infinite motor speed. The maximum speed of the motor is defined by DC-link voltage for machines with FWI larger than one.

The field weakening index is also important from fail operational point of view. One motor sub-system can be field weakened completely ($i_d = -i_{ch}$ ) whereas second sub-system generates the torque. This mechanism can be used during the motor fault. However field weakening index needs to be lower than one. Mutual inductances should be taken into account too.

### *1.2 Distributed winding*

The second possible stator winding arrangement is the distributed winding. Winding is divided into multiple armature slots Sanada and Morimoto (2009). One armature slot can contain coils of different phases or even coils of different sub-systems using this arrangement. Mutual inductances between phases can be higher in compare to non-overlapping concentrated winding arrangement. The distributed winding can be divided into multiple sub-systems to form multiple three-phase systems. Multiple three-phase systems can be created using several methods. Each method has some advantages and disadvantagesWang et al. (2018).

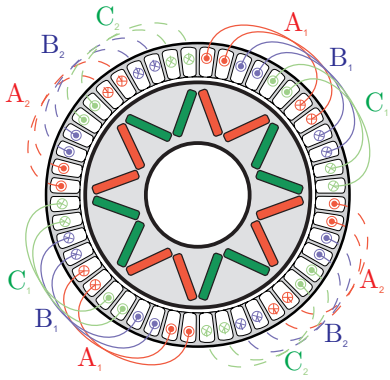


Fig. 3. Double three-phase motor with distributed winding and segregated sub-systems.

Table 1. Fundamental motor parameters.

| Specification | Symbol | Value |
|---|---|---|
| Continuous power | $P_c$ | 120 kW |
| Peak power | $P_{pk}$ | 250 kW |
| Nominal speed | $\omega_n$ | 8000 rpm |
| Maximal speed | $\omega_m$ | 20000 rpm |
| Maximal continuous current | $I_c$ | 120 A (rms) |
| Maximal current for 10 s | $I_m$ | 300 A (rms) |
| Continuous Torque | $T_c$ | 115 N·m |
| Maximal Torque | $T_m$ | 310 N·m |
| Back-EMF constant | $\Psi_m$ | 70 mV/(rad $s^{-1}$) |
| Pole pairs | $Pp$ | 4 |
| Phases | $p_h$ | 6 (2 × ⅄) |

Individual coils can be evenly distributed into multiple sub-systems to form fully symmetrical structure. Coils of different sub-systems are strongly coupled in this case. Mutual inductances between sub-systems are much higher in compare to multiple three-phase structure with non-overlapping concentrated windings. The double three-phase motor with interlaced sub-systems is shown in Figure 2. The motor can operate using only one sub-system without any problems during fault, because individual three-phase sub-systems are symmetrical. Main disadvantage of this structure comes from high mutual inductances between sub-systems. Currents of one sub-system influence the second one. This effect causes problems during motor short circuit faults.

The second method to form multiple three-phase motor uses coil groups. Individual sub-systems are geometrically separated. We can speak about motor with segregated sub-systems in this case. Mutual inductances between sub-systems are lower in compare to mutual inductances between phases within sub-systems. Double three-phase motor with segregated windings is shown in Figure 3. This motor structure can operate during the motor short circuit faults. However control algorithm for this structure is more complex.

Mutual inductances between phases within sub-system are not the same. Mutual inductances between boundary windings ($M_{ac}$) is lower in compare to other inductances within the sub-system ($M_{ab}, M_{bc}$). This asymmetry needs to be taken into account during control algorithm design.

Individual stator structures are compared with each other. Fundamental motor parameters are the same for every

stator coil arrangement. The motor parameters are shown in Table 1. Multiple three-phase motors with these parameters are suitable for automotive industry. Test conditions for individual structures are also the same. Different motor behaviour is caused by different inductances.

## 2. MOTOR WITH INTERLACED WINDINGS AND LOW MUTUAL INDUCTANCES

Low mutual inductances between sub-systems can be reached using non-overlapping concentrated winding. This stator arrangement is shown in Fig. 1.

Inductance fluctuation can be seen in Fig. 4. The fluctuation is caused by the rotor geometry. Mentioned inductance fluctuation leads to different $L_d$ and $L_q$ inductances. Motors with different $dq$ inductances generate reluctance torque. Higher inductance difference leads to higher reluctance torque.

Inductances can be transformed into $dq$ coordinates using extended transformations Miller and McGilp (2009). Inductance fluctualiton is transformed into constants. The $q$ axis inductance is approximately 380 $\mu$H, The $d$ inductance is approximately only 240 $\mu$H. Mutual inductances between sub-systems are roughly 20 % of self inductances. The interaction between sub-systems is low for this reason. Inductances transformed into $dq$ coordinates has zero mutual inductances between $d$ and $q$ axis.

### *2.1 Active short circuit simulations*

The active short circuit mode can be important during motor or inverter faults. For instance one inverter transistor can be short circuited. Damaged phase is subsequently connected to negative or positive DC-link voltage. Other phases of damaged sub-system can be connected to same potential to reduce influence of damaged transistor. The field weakening index of the motor is lower than one so motor currents during ASC are lower than nominal motor currents. This operating mode does not cause thermal damage of the motor.

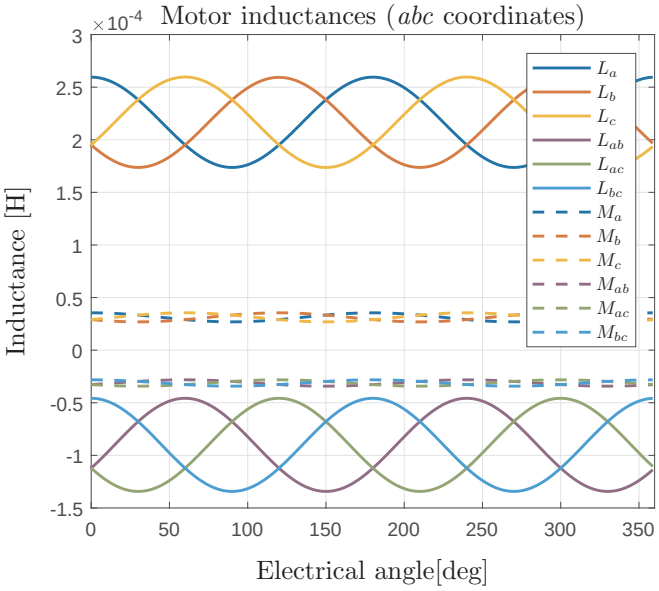


Fig. 4. Inductances of analysed double three-phase motor with low mutual inductances between sub-systems.

ASC currents for double three-phase motor can be calculated from (3). $R_s$ denotes phase winding resistance. Variables $L_d, L_q, M_d, M_q$ represent self inductances and mutual inductances transformed into $dq$ coordinates. $\omega_e$ denotes electrical motor angular speed. The back-EMF constant is reflected by $\Psi_M$. Variables $i$ and $u$ represent current and voltage in $dq$ coordinates.

$$\begin{aligned} u_{d1} &= R_s i_{d1} + L_d \frac{\mathrm{d}i_{d1}}{\mathrm{d}t} + M_d \frac{\mathrm{d}i_{d1}}{\mathrm{d}t} - \omega_e (L_q i_{q1} + M_q i_{q2}) \\ u_{q1} &= R_s i_{q1} + L_q \frac{\mathrm{d}i_{q1}}{\mathrm{d}t} + M_q \frac{\mathrm{d}i_{q2}}{\mathrm{d}t} + \omega_e (\Psi_M + L_d i_{d1} + M_d i_{d2}) \end{aligned} \tag{3}$$

Voltages are equal to zero during ASC. $dq$ currents are function of speed. Steady state currents can be calculated using (4). Variables $i_{d_{ASC\_ALL}}$ and $i_{q_{ASC\_ALL}}$ represent currents of individual sub-systems during full ASC operation. Both sub-systems operate in ASC mode in this case.

$$\begin{aligned} i_{d_{ASC\_ALL}} &= -\frac{\omega_e^2 (L_q + M_q) \Psi_M}{\omega_e^2 (L_d + M_d)(L_q + M_q) + R_s^2} \\ i_{q_{ASC\_ALL}} &= -\frac{R_s \omega_e \Psi_M}{\omega_e^2 (L_d + M_d)(L_q + M_q) + R_s^2} \end{aligned} \tag{4}$$

However, only one sub-system can be switched into ASC mode using double three-phase arrangement. In this case ASC current of one subsystem can be calculated using (5). Variables $i_{d_{ASC}}$ and $i_{q_{ASC}}$ denote currents of ASC subsystem. Currents of second sub-system are represented by variables $i_{d_{ASC}}$ and $i_{q_{ASC}}$.

$$\begin{aligned} i_{d_{ASC}} &= \frac{R_s \omega_e M_q i_{q_{RUN}} - \omega_e^2 L_q (M_d i_{d_{RUN}} + \Psi_M)}{\omega_e^2 L_d L_q + R_s^2} \\ i_{q_{ASC}} &= -\frac{R_s \omega_e (M_d i_{d_{RUN}} + \Psi_M) + \omega_e^2 L_d M_q i_{q_{RUN}}}{\omega_e^2 L_d L_q + R_s^2} \end{aligned} \tag{5}$$

Motor torque during operation with one ASC sub-system can be calculated using (6). Variables $i_{d_{RUN}}$ and $i_{q_{RUN}}$ denote currents of active sub-system.

$$\begin{aligned} T_{mot} = \frac{3}{2} Pp ( & \Psi_M (i_{q_{RUN}} + i_{q_{ASC}}) + \\ & + (i_{d_{RUN}} i_{q_{RUN}} + i_{d_{ASC}} i_{q_{ASC}})(L_d - L_q) + \\ & + (i_{d_{RUN}} i_{q_{ASC}} + i_{d_{ASC}} i_{q_{RUN}})(M_d - M_q)) \end{aligned} \tag{6}$$

Motor ASC currents $i_{d_{ASC}}$ and $i_{q_{ASC}}$ are shown in Fig. 5. The amplitude of phase currents is almost 160 A in this case. This value represents approximately 113 A rms. Table 1 defines maximum continuous current to 120 A. The motor can operate continuously in this mode.

The mutual influence between sub-systems reduces Back-EMF voltage of second sub-system. Amplitude of back-EMF voltage at 5000 rpm is approximately 90 V during all phase open simulation. However, back-EMF voltage of APO sub-system is reduced by ASC currents to aproximatelly 75 V.

On the other hand, ASC currents are influenced by running sub-system during operation with one ASC subsystem. This influence can be determined by (7) during high speed operation.

$$\begin{aligned} \lim_{\omega_e \to \infty} i_{d_{ASC}} &= -\frac{M_{dd} i_d^{s_2} + \Psi_M}{L_{dd}} \\ \lim_{\omega_e \to \infty} i_{q_{ASC}} &= -\frac{M_{qq} i_q^{s_2}}{L_{qq}} \end{aligned} \tag{7}$$

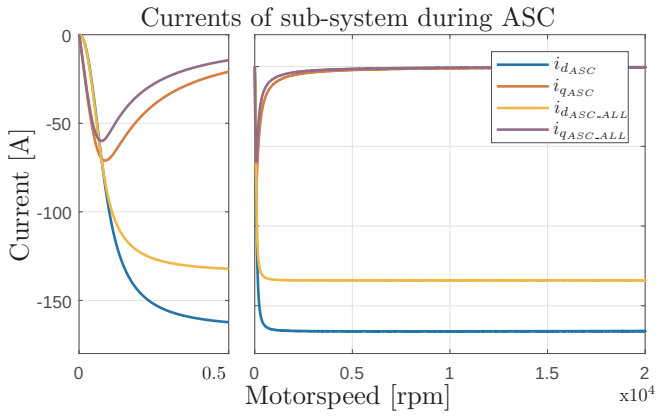


Fig. 5. $dq$ currents of ASC sub-system.

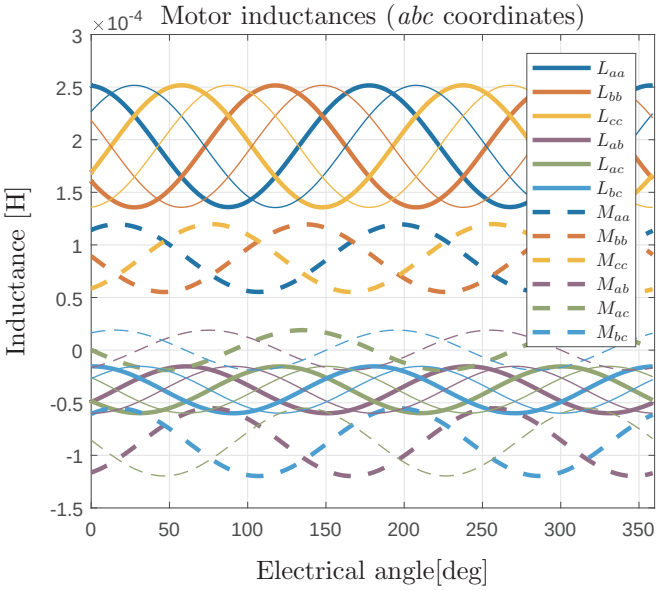


Fig. 6. Inductances of double three-phase motor with high mutual inductances between sub-systems.

Mutual inductance between sub-systems can reduce currents of ASC currents. However breaking torque generated by $i_{q_{ASC}}$ can be increased with increasing generated torque.

The whole motor can be switched into ASC too. In this case, ASC currents of one sub-system are reduced due to mutual inductances. The currents $i_{d_{ASC\_ALL}}$ and $i_{q_{ASC\_ALL}}$ are shown in Fig. 5. Their value during high speed operation can be calculated using (8).

$$\begin{aligned} \lim_{\omega_e \to \infty} i_{d_{ASC\_ALL}} &= -\frac{\Psi_M}{(L_{dd} + M_{dd})} \\ \lim_{\omega_e \to \infty} i_{q_{ASC\_ALL}} &= 0 \end{aligned} \tag{8}$$

Motor current amplitude is reduced to approximately 130 A. This value represents roughly 90 A rms.

## 3. MOTOR WITH INTERLACED WINDINGS AND HIGH MUTUAL INDUCTANCES

High mutual inductances between motor parts is a typical feature of motors with distributed winding arrangement and interlaced sub-systems. This stator arrangement is shown in Fig. 2. Coils of individual sub-systems overlap each other. There is strong magnetic coupling between coils for this reason.

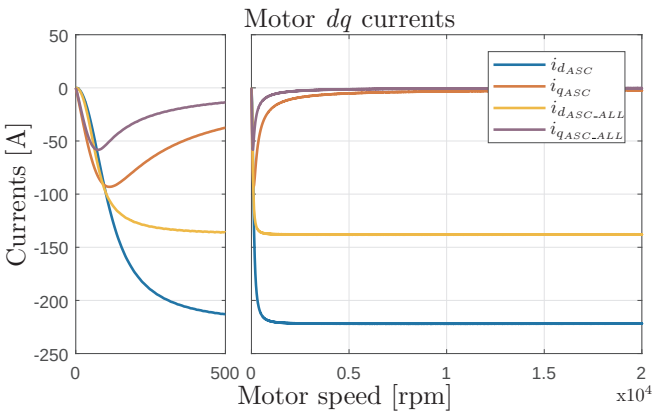


Fig. 7. Motor currents during ASC in both sub-systems

All motor inductances are shown in Fig. 6. Inductances visualised by thick curves represent inductances related to first sub-system. Thin curves denote inductances related to second sub-system. Inductances reflect phase shift between sub-systems caused by mechanical arrangement.

Inductances can be transformed into $dq$ coordinates. Transformation principe for multiple three-phase motors is described in detail in Kozovsky et al. (2016) .The phase shift between sub-systems is taken into account by transformation. The motor is fully symmetrical and inductances are transformed into constants. The $q$ axis inductance is approximately 290 $\mu$H, The $d$ inductance is approximately only 180 $\mu H$. Inductances transformed into $dq$ coordinates has zero mutual inductances between $d$ and $q$ axis. Nonzero mutual inductance between $d$ and $q$ axis is typical for motors with phase shift between sub-systems.

Mutual inductances represent approximately 65 % of self inductances. Mutual inductances fluctuation is significantly higher compared to non-overlapping concentrated winding arrangement. The interaction between sub-systems is also high and needs to be considered.

The electrical angle between sub-systems is 30 degrees. Back-EMF constant is equal for each coil arrangement. Amplitude of back-EMF voltage is the same as in previous arrangement for this reason.

### *3.1 Active short circuit simulations*

Simulation results of the motor switched into ASC are almost the same in compare to previously analysed arrangement. This behaviour is caused by the same sum of mutual and self inductances in all arrangements. Equation (5) can be used to calculate ASC currents also for this arrangement because mutual inductance between $d$ and $q$ axis is zero. Motor currents are shown in Fig. 7.

The main difference between arrangements can be seen during ASC of one sub-system. Coils of one sub-system are evenly distributed over entire stator surface as it can be seen in Fig. 2. Inductances of one sub-systems are lower in compare to other arrangements.

The amplitude of ASC current is roughly 220 A (see Fig. 7). This value represents approximately 155 A rms. This

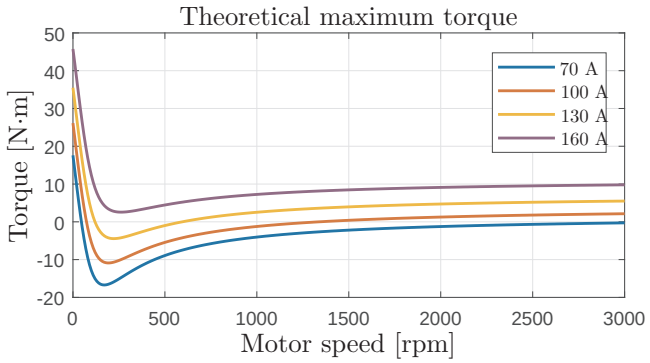


Fig. 8. Theoretical maximum motor torque (one sub-system active and second sub-system in ASC).

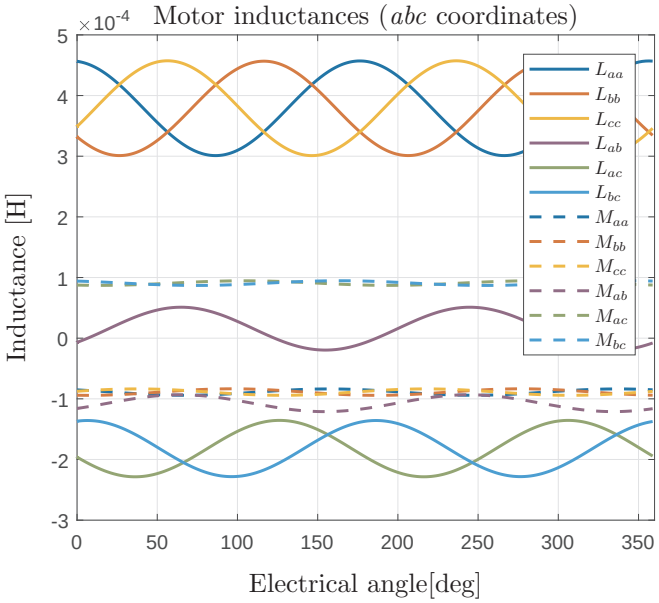


Fig. 9. Inductances of double three-phase motor with segregated sub-systems

value is higher than maximum continuous current. Motor cannot operate in this mode continuously.

Another disadvantage of this arrangement comes from field weakening of the whole motor. Theoretical maximum torque of the motor during ASC of one sub-system can be calculated using (6).

ASC currents of one sub-system depend on currents of active sub-system. Maximum motor torque for different phase currents of second sub-system is shown in Fig. 8. Field weakening angle was configured to reach maximum torque using defined current amplitude.

## 4. MOTOR WITH SEGREGATED WINDINGS

High mutual inductances between motor parts can be reduced using segregated structure. The segregated structure is shown in Fig. 3. The mutual inductance between sub-systems is significantly reduced by geometrical displacement. Individual sub-systems are completely geometrically separated. Fault caused by electrical short-circuit between sub-systems does not occur in this case. However there is a strong magnetic coupling between phases within sub-system.
Inductances of double three-phase motor with segregated

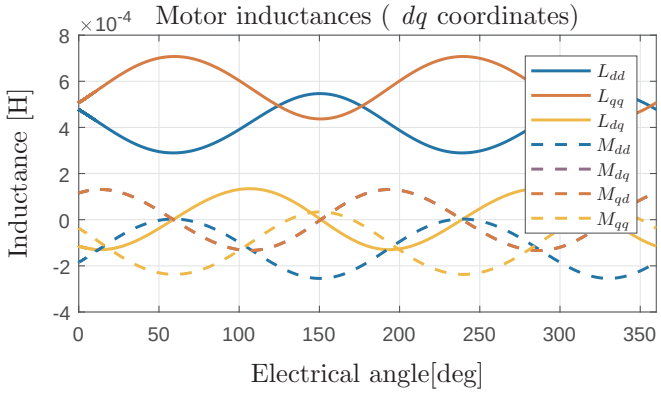


Fig. 10. Inductances of double three-phase motor with segregated sub-systems transformed into $dq$ coordinates.

windings are shown in Fig. 9. Inductances of one sub-system are not symmetrical in contradistinction to previous structures. The transformation into $dq$ coordinates can be realised, however inductances transformed into $dq$ coordinates are not constant. Inductances transformed into $dq$ coordinates are shown in Fig. 10.

The motor behaviour during the normal operation is symmetrical because the sum of self inductances and mutual inductances in $dq$ coordinates is constat. However behaviour of this structure is problematic during the fault.

### *4.1 Active short circuit simulations*

The whole motor can be switched into ASC. The behaviour is almost the same in compare to previous structures. ASC current can be seen in Figure 12. If both sub-systems are switched into ASC, equation (5) can be used to calculate motor currents.

Problematic behaviour is caused by asymmetrical inductances within sub-system. Motor can operate using only one sub-system but special control algorithm to compensate inductance asymmetry must be used.

One sub-system can be switched into all phase open (APO) mode during some faults. The control algorithm must compensate inductance asymmetry. Elliptical voltage vector trajectory can be used instead of classical circular voltage vector trajectory which is normally used for three phase motors.

Damaged sub-system can be switched into ASC mode too. Currents during ASC of one sub-system can be sees in Fig. 12. Current oscillations generate unwanted torque ripples. The current oscillations affect second sub-system. The back-EMF voltage is affected by ASC sub-system. Back-EMF voltage of second sub-system is shown in Fig. 11.

## 5. CONCLUSION

This paper demonstrates behaviour differences of typical-double three-phase motor arrangements. The most suitable motor arrangement is the structure with low mutual inductances between sub-systems. The control algorithm for classical three-phase motors can be used for individual sub-systems.

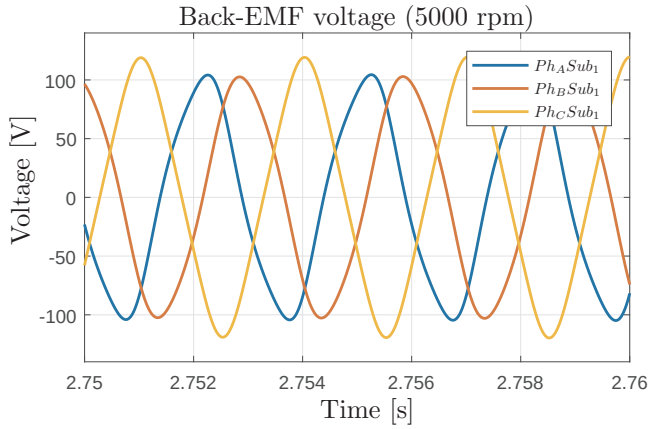


Fig. 11. Back-EMF phase voltage of double three-phase motor with phase shift between sub-systems.

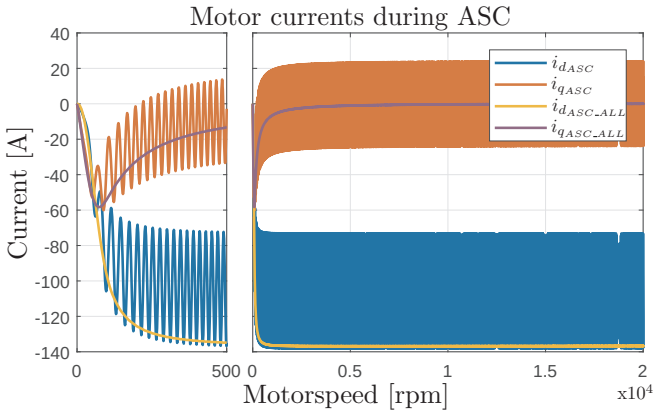


Fig. 12. *dq* currents of ASC sub-system.

The motor with high mutual inductances between subsystems is not suitable for fail operation applications. Problems with strong magnetic coupling between subsystems can't be solved by control algorithm. The torque limitation of the whole structure is mathematically derived and also simulated.

Last analysed structure with segregated subsystem can be used for fail operation application. However specialised control algorithm to compensate influence of motor asymmetry must to be used. Mechanical arrangement of the motor reduces the probability of short circuit between subsystems. This fact is one of the main advantages of this arrangement.

## ACKNOWLEDGEMENTS

The research was supported by ECSEL JU under the project H2020 737469 AutoDrive - Advancing fail-aware, fail-safe, and failoperational electronic components, systems, and architectures for fully automated driving to make future mobility safer, affordable, and end-user acceptable.

The completion of this paper was made possible by the grant No. FEKT-S-17-4234 - Industry 4.0 in automation and cybernetics" financially supported by the Internal science fund of Brno University of Technology.

This research was carried out under the project CEITEC 2020 (LQ1601) with financial support from the Ministry of Education, Youth and Sports of the Czech Republic under the National Sustainability Programme II.

## REFERENCES

Chong, L., Dutta, R., Dai, N.Q., Rahman, M.F., and Lovatt, H. (2010). Comparison of concentrated and distributed windings in an IPM machine for field weakening applications. In *2010 20th Australasian Universities Power Engineering Conference*, 1–5. IEEE.

Dhulipati, H., Mukundan, S., Iyer, K.L.V., and Kar, N.C. (2017). Skewing of stator windings for reduction of spatial harmonics in concentrated wound PMSM. *Canadian Conference on Electrical and Computer Engineering*. doi:10.1109/CCECE.2017.7946834.

EL-Refaie, A.M. (2010). Fractional-slot concentrated-windings synchronous permanent magnet machines: Opportunities and challenges. *IEEE Transactions on Industrial Electronics*, 57(1), 107–121. doi: 10.1109/TIE.2009.2030211.

Giangrande, P., Madonna, V., Nuzzo, S., Gerada, C., and Galea, M. (2019). Braking Torque Compensation Strategy and Thermal Behavior of a Dual Three-Phase Winding PMSM During Short-Circuit Fault. In *2019 IEEE International Electric Machines & Drives Conference (IEMDC)*, 2245–2250. IEEE. doi: 10.1109/iemdc.2019.8785164.

Kozovsky, M., Blaha, P., and Vaclavek, P. (2016). Verification of nine-phase PMSM model in d-q coordinates with mutual couplings. In *2016 6th IEEE International Conference on Control System, Computing and Engineering (ICCSCE)*, 73–78. IEEE. doi: 10.1109/ICCSCE.2016.7893548.

Miller, T. and McGilp, M. (2009). Analysis of multi-phase permanent-magnet synchronous machines. In *2009 International Conference on Electrical Machines and Systems*, 1–6. IEEE. doi:10.1109/ICEMS.2009.5382988.

Pouramin, A., Ekanayake, S., Dutta, R., and Rahman, M.F. (2017). Challenges for including characteristic current as a design parameter in optimization of IPM machines. In *2017 IEEE International Electric Machines and Drives Conference, IEMDC 2017*, 1–6. IEEE. doi:10.1109/IEMDC.2017.8002184.

Sanada, M. and Morimoto, S. (2009). Efficiency improvement at high-speed operation using large air-gap configuration for PMSM. In *2008 18th International Conference on Electrical Machines*, 1–6. IEEE. doi: 10.1109/icelmach.2008.4799932.

Wang, B., Wang, J., Sen, B., Griffo, A., Sun, Z., and Chong, E. (2018). A Fault-Tolerant Machine Drive Based on Permanent Magnet-Assisted Synchronous Reluctance Machine. *IEEE Transactions on Industry Applications*, 54(2), 1349–1359. doi: 10.1109/TIA.2017.2781201.

Yepes, A.G., Doval-Gandoy, J., Baneira, F., Perez-Estevez, D., and Lopez, O. (2017). Current Harmonic Compensation for *n*-Phase Machines With Asymmetrical Winding Arrangement and Different Neutral Configurations. *IEEE Transactions on Industry Applications*, 53(6), 5426–5439. doi:10.1109/TIA.2017.2722426.